Published in final edited form as:
Stem Cells. 2008 May ; 26(5): 1337–1346. doi:10.1634/stemcells.2008-0053.

Conditional Stabilization of β-Catenin Expands the Pool of Lung Stem Cells

Susan D. Reynolds[a], **Anna C. Zemke**[a], **Adam Giangreco**[a], **Brian L. Brockway**[a], **Roxana M. Teisanu**[a], **Jeffrey A. Drake**[a], **Thomas Mariani**[b], **Peter Y.P. Di**[a], **Mark M. Taketo**[c], and **Barry R. Stripp**[a]

[a]Center for Lung Regeneration, Department of Environmental and Occupational Health, University of Pittsburgh, Pittsburgh, Pennsylvania, USA

[b]Division of Pulmonary Medicine, Brigham and Women's Hospital, Harvard Medical School, Boston Massachusetts, USA

[c]Department of Pharmacology, Graduate School of Medicine, Kyoto University, Kyoto, Japan

Abstract

Maintenance of classic stem cell hierarchies is dependent upon stem cell self-renewal mediated in part by Wnt/β-catenin regulation of the cell cycle. This function is critical in rapidly renewing tissues due to the obligate role played by the tissue stem cell. However, the stem cell hierarchy responsible for maintenance of the conducting airway epithelium is distinct from classic stem cell hierarchies. The epithelium of conducting airways is maintained by transit-amplifying cells in the steady state; rare bronchiolar stem cells are activated to participate in epithelial repair only following depletion of transit-amplifying cells. Here, we investigate how signaling through β-catenin affects establishment and maintenance of the stem cell hierarchy within the slowly renewing epithelium of the lung. Conditional potentiation of β-catenin signaling in the embryonic lung results in amplification of airway stem cells through attenuated differentiation rather than augmented proliferation. Our data demonstrate that the differentiation-modulating activities of stabilized β-catenin account for expansion of tissue stem cells.

Keywords

Adult stem cells; Progenitor cells; Regeneration; Bronchiole; Transgenic mouse

Introduction

The epithelium lining conducting airways turns over slowly in the steady state yet has significant reparative capacity that is activated following injury [1–5]. Cell-selective injury models have been used to identify reparative cells and stratify them according to their mitotic and differentiation potentials. Nonciliated bronchiolar Clara cells function as a facultative progenitor for maintenance of the epithelium of the adult mouse lung both in the steady state and during repair following injury that specifically targets postmitotic ciliated cells [4,5]. However, the metabolic functions of quiescent Clara cells (similar to liver hepatocytes [6] and pancreatic β-cells [7]) render them susceptible to xenobiotic agents such as naphthalene [8].

Correspondence: Barry R. Stripp, Ph.D., 2075 MSRBII, 106 Research Drive, DUMC Box 103000, Durham, North Carolina 27710, USA. Telephone: 919-668-7762; Fax: 919-684-5266; barry.stripp@duke.edu.

Disclosure of Potential Conflicts of Interest: The authors indicate no potential conflicts of interest.

In mice, naphthalene exposure results in a dose-dependent depletion of the Clara cell population [9] and activation of a population of rare, naphthalene-resistant, spatially restricted cells that proliferate in response to injury [10]. Genetic ablation studies defined the naphthalene-resistant cell as the highest-ranking member of a bronchiolar stem cell hierarchy [3]. Bronchiolar tissue stem cells (TSC) are restricted to two discrete microenvironments, the neuroepithelial body and the bronchoalveolar duct junction [2,3,11]. In agreement with their naphthalene-resistant phenotype, neuroepithelial body-associated TSC express less of the naphthalene-metabolizing enzyme cytochrome P450-2F2 (CyP450-2F2) [11]. Both bronchiolar TSC and the Clara cell express the secretory cell marker Clara cell secretory protein (CCSP) [3]. However, TSC may be distinguished from Clara cells on the basis of their coexpression of Surfactant protein-C (SP-C), a gene expressed within endodermal precursor cells of the developing lung and alveolar type 2 cells of the adult [12,13].

Cell maintenance in slowly renewing tissues is thought to be different from that occurring within rapidly renewing tissues. Rapidly renewing tissues, such as the epithelium of the small intestine and the cellular components of the hematopoietic system, are maintained by classic stem cell hierarchies. In these hierarchies, rare tissue stem cells give rise to one or more populations of abundant transit-amplifying cells (TAC). These TAC are responsible for the generation of sufficient differentiating progeny for maintenance of some or all components of the tissue in which they reside [14,15]. Principal differences between rapidly and slowly renewing tissues relate to the frequency with which TSC and TAC cycle in the steady state and the differentiated status of the TAC population. Transit-amplifying cells of the small intestine proliferate continuously, lack differentiated character, and are spatially separated from their differentiated derivatives that either line the villus or migrate to the crypt base. In contrast, the bronchiolar TAC is thought to be a differentiated secretory (Clara) cell that is normally quiescent but responds to injury by dividing, self-renewing, and giving rise to progeny that differentiate into one or more cell types (ciliated cells and Clara cells). Thus, intestinal TAC are dedicated progenitor cells, whereas TAC of the lung and other slowly renewing organs behave as facultative progenitor cells. In light of these functional distinctions between the stem cell hierarchies of rapidly versus slowly renewing tissues, it is not clear whether molecular signaling mechanisms that regulate one type of hierarchy can be extrapolated to other types of reparative systems.

Genetic perturbations resulting in the stabilization of cytoplasmic β-catenin within the proliferative fraction of intestinal epithelial cells lead to uncontrolled expansion of cells that are unable to generate differentiating postmitotic progeny and have properties similar to the TSC [16,17]. Potentiation of the Wnt/β-catenin pathway has similarly profound influences on the self-renewal capacity and differentiation potential of other stem cell hierarchies, such as those of the hematopoietic system [18–21] or the epidermis [22–25], leading in each case to expansion of the TSC/TAC pool and either arrested or altered differentiation. However, even though the Wnt/β-catenin pathway plays a critical role in regulation of lung development [26–28], it is unclear whether it fulfills roles in the maintenance of adult lung stem cells similar to those of more rapidly renewing organs.

In this study, we established that β-catenin-mediated signaling, which is active in early lung endoderm, is extinguished within the differentiating epithelium. Constitutive potentiation of β-catenin signaling within the developing lung endoderm at mouse embryonic day 16.5 arrests epithelial maturation and leads to expansion of the bronchiolar stem cell pool in adult airways. These supernumerary bronchiolar stem cells displayed a normal proliferative response to injury and returned to a quiescent state upon epithelial restitution. These findings suggest that downregulation of Wnt/β-catenin signaling is necessary for stratification of the bronchiolar stem cell hierarchy and that stabilization of β-catenin interferes with the establishment of the transit-amplifying pool and differentiated cell types.

Materials and Methods

Animal Husbandry

Colonies of wild-type and genetically modified mice (supplemental online Table 1) were maintained as in-house breeding colonies under specific pathogen-free conditions in an Association for Assessment and Accreditation of Laboratory Animal Care-accredited facility. Experiments involving adult mice were performed with animals between 2 and 4 months of age.

Naphthalene Administration

Naphthalene administration was carried out as previously described, with doses adjusted according to strain to achieve a >90% decrease in the abundance of CCSP and CyP450-2F2 mRNA in total lung RNA of wild-type mice [10].

Bromodeoxyuridine Administration

For continuous labeling studies, bromodeoxyuridine (BrdU; Sigma-Aldrich, St. Louis, http://www.sigmaaldrich.com) in sterile saline (20 mg/ml) was delivered using a 14-day mini-osmotic pump (Alzet 2002; Durect, Cupertino, CA, http://www.alzet.com). Pumps were implanted 24 hours after naphthalene exposure. For measurement of the instantaneous proliferative index of epithelial cells in vivo, proliferating cells were pulse-labeled through intraperitoneal injection of BrdU (50 mg/kg body weight; Sigma-Aldrich) 2 hours prior to sacrifice.

Tissue Recovery

The trachea was cannulated, and the left lobe was removed and homogenized for RNA isolation [29]. For standard light microscopy, right lung lobes were inflation-fixed with 10% neutral buffered formalin for 2 hours. For ultrastructural analysis, tissue was inflation-fixed as indicated above with 2.5% glutaraldehyde in phosphate-buffered saline (PBS).

Immunofluorescence

Immunofluorescence techniques were used to detect antigens listed in supplemental online Table 2. Primary antibodies were diluted in 5% BSA/PBS at the concentrations listed in supplemental online Table 2. Antigen-antibody complexes were visualized using an Olympus Fluoview confocal microscope using 2 μg/ml 4,6-diamidino-2-phenylindole (Sigma-Aldrich) in mounting medium as the counterstain.

Transmission Electron Microscopy

Tissue was processed for transmission electron microscopy according to previously published methods [31] and examined using a Jeol 1011 transmission electron microscope (Jeol, Peabody, MA, http://www.jeolusa.com).

Morphometric Analysis

Cell Density Analysis—The length of the bronchiolar and terminal bronchiolar epithelium was determined using the measurement function of Image-Pro Plus (Media Cybernetics, Silver Spring, MD, http://www.mediacy.com). Cell density was determined by counting nucleated cells in this region and is expressed as cells per millimeter of basement membrane.

Proliferative Index Analysis—The proliferative index was defined as the number of BrdU-labeled nuclei divided by the total number of nuclei and is presented as a percentage. Representation of cells within the proliferative pool was defined as the number of cells that

coexpressed a lineage marker (CCSP, CGRP, or FoxJ1) and BrdU divided by the total number of BrdU-positive cells.

RNA Abundance

Quantitative reverse transcription (RT)-polymerase chain reaction (PCR) was used to assess mRNA abundance. Total RNA was prepared from the left lung lobe as previously described [10]. cDNA was prepared and assayed as previously described [32] using Assays-on-Demand gene expression probe/primer sets from Applied Biosystems (Foster City, CA, http://www.appliedbiosystems.com). Expression was quantified using an ABI Prism 7000 Sequence Detection System (Applied Biosystems), and values were calculated by the $\Delta\Delta C_T$ method using a standard total lung RNA preparation as the calibrator [33].

Clonogenic Frequency Analysis

Airway cells were prepared by the method of Chichester et al. [34]. CD45-positive cells were depleted using Dynabeads (Dynal M-280; Dynal Biotech, Carlsbad, CA, http://www.invitrogen.com/dynal) and biotinylated anti-CD45 according to the manufacturer's directions. Clonogenic frequency within CD45(–) airway cell preparations was determined by the method of Taswell [35]. Cells were cultured in mouse tracheal epithelial medium [36] at 5% CO_2, 37°C for 1 week.

Results

β-Catenin Signaling During Airway Development

Airway secretory cell differentiation proceeds in a proximal-to-distal wave and is completed in the terminal bronchiole during the postnatal period [13,37,38]. Later stages of embryonic lung development were characterized by a restriction of prosurfactant protein C (proSPC) expression to the epithelium lining terminal lung buds and an increase in expression of CCSP in future terminal bronchioles residing immediately proximal to distal lung buds (supplemental online Fig. 1). In contrast with previous reports [39], these antigens were expressed in distinct cell types of the embryonic lung. By postnatal day 2, terminal bronchioles included a subset of epithelial cells expressing both CCSP and proSPC antigens. This change was transient, and CCSP/proSPC dual-positive cells were observed only in rare cell types at the bronchoalveolar duct junction after postnatal day 2 (supplemental online Fig. 1).

The relationship between secretory differentiation and *β*-catenin signaling was determined at day post coitum (dpc) 18.5 by colocalization CCSP with expression of the *β*-catenin reporter transgene TOPGal. TOPGal transgene activity was measured through X-gal histochemical staining of the *β*-galactosidase (*β*-gal) reporter gene [40]. At this time, the bronchial epithelium expressed CCSP and was negative for *β*gal activity (supplemental online Fig. 2). In contrast, the distal airway epithelium was in transition. CCSP-immunoreactive terminal bronchioles were *β*gal-negative, whereas regions that were CCSP-negative exhibited high levels of *β*gal activity. This analysis indicated that CCSP and the TOPGal transgene were expressed in reciprocal patterns and suggested that establishment of the airway secretory lineage, like that of other cell types of the maturing lung endoderm, was regulated by Wnt/*β*-catenin signaling.

Stabilization of *β*-Catenin Within the Airway Epithelium Blocks Clara Cell Differentiation

Stabilization of β-Catenin Attenuates Airway Epithelial Cell Differentiation— Efficient and airway-specific recombination of the ROSA26-floxed STOP-LacZ (ROSA26-RS [41]) and $Catnb^{floxE3}$ [42] alleles was observed in mice expressing Cre recombinase under regulation of the CCSP promoter (CCSP-Cre transgene [43] (supplemental online Figs. 3, 4). Use of the ROSA26-RS Cre reporter indicated that recombination first occurred at embryonic

day 16.5 and proceeded through the early postnatal period (supplemental online Fig. 3). Comparative morphological analysis of the adult conducting airway epithelium in wild-type and Catnb$^{\Delta E3}$ mice suggested that stabilization of *β*-catenin altered the molecular characteristics of steady-state secretory cells (Fig. 1). In contrast with wild-type CCSP-expressing cells, recombined cells of the Catnb$^{\Delta E3}$ airway exhibited weak CCSP immunofluorescence and an unusual low cuboidal to squamous morphology. Transmission electron microscopic analysis of adult wild-type bronchioles detected nonciliated Clara cells characterized by their domed morphology, a high cytoplasmic-to-nuclear ratio, and an abundance of cytoplasmic organelles, including mitochondria, secretory granules, and endoplasmic reticulum (Fig. 1). In contrast, the majority of nonciliated cells within bronchioles of Catnb$^{\Delta E3}$ mice exhibited a low cuboidal shape, a low cytoplasmic-to-nuclear ratio, and an accompanying reduction in cytoplasmic organelles. Abundant glycogen granules, a hallmark of embryonic airway cells, were absent from nonciliated airway cells of adult wild-type or Catnb$^{\Delta E3}$ mice. These data demonstrated that nonciliated airway cells of Catnb$^{\Delta E3}$ mice were undifferentiated relative to epithelial cells at this airway location in wild-type mice.

Qualitative changes to Catnb$^{\Delta E3}$ secretory cells identified by immunofluorescent staining were quantified through analysis of two secretory cell-specific mRNAs, CCSP and CyP450-2F2, within total lung RNA (Fig. 2). CCSP (wild-type [WT] vs. heterozygous [het], $p = .001$; WT vs. homozygous [homo], $p = .0003$) and CyP450-2F2 (WT vs. het, $p = .0003$; WT vs. homo, $p = .004$) mRNA abundance was significantly decreased in adult lung RNA from mice that were positive for the CCSP-Cre transgene and either homozygous or heterozygous for the *Catnb*$^{flox(E3)}$ allele. Expression of these secretory cell-specific genes did not vary as a function of zygosity (CCSP, $p = .807$; CyP450-2F2, $p = .108$). Abundance of SP-C mRNA, a marker for early lung epithelial progenitor cells and adult alveolar type 2 cells, did not vary between wild-type and heterozygous ($p = .154$) or homozygous ($p = .696$) mice. These data demonstrated that expression of truncated *β*-catenin specifically altered the molecular phenotype of airway secretory cells in the adult lung and that this was a dominant phenotype.

The airway epithelium matures postnatally, a process that is accompanied by induction of genes involved in differentiated functions [44,45]. Quantitative RT-PCR was used to determine whether Catnb$^{\Delta E3}$ lungs progress through this postnatal differentiation process (Fig. 2). In wild-type lung, the abundance of CCSP and CyP450-2F2 mRNAs did not vary between dpc 17.5 and postnatal day (pnd) 1, underwent a statistically significant increase in abundance between pnd 1 and 21 (CCSP: $p < .0001$; CyP450-2F2: $p < .0001$), and was constant between pnd 21 and 48. In lungs of Catnb$^{\Delta E3}$ mice, the abundance of CCSP and CyP450-2F2 mRNAs did not vary between dpc 17.5 and pnd 1 and was indistinguishable from expression levels detected in lungs of wild-type mice. Abundance of both mRNAs increased between pnd 1 and 21 ($p = .002$) but was approximately 30% of that observed in wild-type lung ($p = .0001$). CCSP and CyP450-2F2 mRNA abundance did not vary between pnd 21 and 48 in Catnb$^{\Delta E3}$ mice, and the expression level was significantly different from that of wild-type (CCSP, $p = .008$; CyP450-2F2, $p = .012$). Similar genotype-dependent differences in expression of additional Clara cell-specific markers were noted (supplemental online Fig. 5). These results were in agreement with the histological demonstration of reduced CCSP protein levels in Catnb$^{\Delta E3}$ airways and indicated that stabilization of *β*-catenin in airway secretory cells attenuated the normal program of postnatal differentiation.

Previous studies involving potentiation of *β*-catenin signaling in the early embryonic lung epithelium demonstrated metaplasia to a mucus cell phenotype [46] or transdetermination to a gut phenotype [26]. In the present model, genotype-dependent differences in expression of gut genes, including MUC2 and TFF3, or the mucus cell gene product Muc5AC were not observed (supplemental online Fig. 6). Similarly, analysis of metaplasia through staining of lung tissue with periodic acid Schiff reagent failed to detect evidence of mucus cells in either

strain of mice (data not shown). These data support the conclusion that stabilization of *β*-catenin affects airway epithelial cell differentiation without altering specification of the bronchiolar lineage.

Truncation of β-Catenin Does Not Alter Airway Cell Density or Proliferation— Expression of an N-terminally truncated form of *β*-catenin has been associated with hyperplasia and tumorigenesis [46]. However, histomorphometric analysis failed to detect alterations in epithelial cell density in the present model system (Fig. 3). To determine whether proliferation was altered, the cumulative proliferative index for conducting airway epithelial cells was determined. Continuous labeling of proliferating cells over a 7-day period was chosen in preference to pulse labeling because of the very low rate of proliferation typically observed in the conducting airway epithelium of the steady-state adult lung [47]. The cumulative proliferative index for the wild-type and Catnb$^{\Delta E3}$ epithelium was 1.20 ± 0.70 and 2.02 ± 0.47, respectively (Fig. 3). These values were indistinguishable by Student's *t* test ($p = .67$) and demonstrated that stabilization of *β*-catenin did not affect airway epithelial proliferation in the steady state. These data are consistent with an absence of tumors in more than 500 Catnb$^{\Delta E3}$ mice bred to date and suggest that expression of N-terminally truncated *β*-catenin does not predispose cells to transformation.

Increased Number of Clonogenic Cells—Molecular and ultrastructural characteristics of Catnb$^{\Delta E3}$ airway cells were similar to that of neuroepithelial body-associated Clara-like cells [48] and the mitotically active facultative progenitor cell, the type A Clara cell [4]. Since stem and transit-amplifying cells have been distinguished on the basis of colony formation in vitro [49–51], we determined the clonogenic frequency of wild-type and Catnb$^{\Delta E3}$ epithelial cells. This analysis (Fig. 3) demonstrated an approximately fourfold increase in colony-forming cells in airways of Catnb$^{\Delta E3}$ mice relative to wild-type controls ($p = .001$). This finding suggested that the available pool of tissue stem cells was increased in airways of Catnb$^{\Delta E3}$ mice.

Stabilization of *β*-Catenin Blocks Clara to Ciliated Cell Differentiation

Ciliated cells arise through two mechanisms. During lung development, ciliated cells may be specified directly from endodermal progenitor cells [52]. In contrast, nascent ciliated cells of the adult bronchiole are generated through differentiation of daughter cells of the facultative progenitor cell [4,5]. The developmental appearance of ciliated cells occurs in a proximal-to-distal gradient that initiates on dpc 14.5 and is essentially complete by approximately dpc 16. After this time, bronchiolar ciliated cells are maintained through proliferation and differentiation of Clara cells. Qualitative analysis of the Catnb$^{\Delta E3}$ epithelium suggested that ciliated cells were under-represented in the adult Catnb$^{\Delta E3}$ epithelium (Fig. 4) To quantify this observation and to determine the cellular basis for the apparent deficiency of ciliated cells, the abundance of FoxJ1 mRNA in wild-type and Catnb$^{\Delta E3}$ lung tissue was determined. Genotype-dependent differences in FoxJ1 message abundance were not observed at either dpc 17.5 or pnd 1 (Fig. 4). These results suggested that specification of the endodermal progenitor was not altered in the context of *β*-catenin stabilization. Analysis of FoxJ1 expression in wild-type weanling and adult mice demonstrated a significant increase in mRNA levels between days 21 and 48 ($p = .042$). In contrast, FoxJ1 mRNA levels decreased in Catnb$^{\Delta E3}$ between pnd 1 and 21 ($p = .0001$) and did not change between pnd 21 and 48. FoxJ1 mRNA levels in wild-type and Catnb$^{\Delta E3}$ lung were significantly different on pnd 21 ($p = .0001$) and in adults ($p = .02$). Demonstration of normal epithelial proliferation (Fig. 3) in combination with underexpression of FoxJ1 mRNA (Fig. 4) in the adult airway supported the conclusion that stabilization of *β*-catenin in CCSP-expressing cells altered the ability of their daughter cells to initiate or progress through the ciliated cell differentiation program.

Stabilization of β-Catenin Enhances Epithelial Reparative Capacity in Bronchioles

Rapid Epithelial Repair Following Naphthalene-Mediated Injury—The impact of β-catenin stabilization on airway epithelial injury and repair was assessed using the naphthalene model of lung injury [10]. Immunofluorescence staining for CCSP and proSPC on recovery day 3 suggested significant differences in the reparative capacity of wild-type and $Catnb^{\Delta E3}$ airways (Fig. 5). CCSP-immunoreactive cells within the wild-type epithelium were detected as discrete foci of nascent cells on recovery day 3. Such regenerative zones were typically 3–5 cell diameters in length. Cells within repairing zones of the wild-type epithelium did not express detectable proSPC. In contrast, the $Catnb^{\Delta E3}$ epithelium was characterized by large stretches of $CCSP^{Lo}$ cells separated by small zones of squamous epithelium. Nearly all $CCSP^{Lo}$ cells coexpressed proSPC, although intensities varied from barely detectable to levels equivalent to that observed in alveolar type 2 cells. ProSPC antigen was nonuniformly distributed within the cytoplasm of dual-positive cells; however, lamellar bodies, indicative of mature alveolar type 2 cells, were not observed (data not shown).

Quantitative PCR analysis of CCSP and CyP450-2F2 mRNA abundance was used to assess the extent of naphthalene-mediated injury and the rate of epithelial repair in the whole lung (Fig. 5). In wild-type mice, CCSP mRNA levels decreased to 12.67% ± 5.48% of steady-state levels 3 days postexposure and recovered to 29.25% ± 14.62% steady-state levels by day 8 of recovery. This level of CCSP depletion and recovery is in agreement with a previous analysis of naphthalene-mediated injury and repair [10]. In contrast, CCSP mRNA levels in the $Catnb^{\Delta E3}$ lung decreased to 24.69% ± 5.22% of steady-state levels on recovery day 3 and recovered to 70.97% ± 14.54% of steady-state levels on day 8. Similar results were noted for CyP450-2F2 (Fig. 5). Consistent with the finding that expression of truncated β-catenin in CCSP-expressing cells attenuated postnatal acquisition of secretory and metabolic functions (Figs. 1, 2, 4; supplemental online Figs. 4, 5), the naphthalene challenge studies provided evidence that stabilization of β-catenin attenuated the xenobiotic metabolizing capacity of $Catnb^{\Delta E3}$ airway secretory cells and resulted in functional enrichment of naphthalene-resistant cells.

Increased Abundance of Naphthalene-Resistant Reparative Cells—Pulse BrdU-labeling techniques were used to determine the kinetics of proliferation in the wild-type and $Catnb^{\Delta E3}$ epithelium. The instantaneous proliferative index for wild-type and $Catnb^{\Delta E3}$ epithelium was indistinguishable in control animals ($p = .36$) and reinforced the previous observation that truncated β-catenin did not affect steady-state proliferation. Analysis of wild-type bronchiolar and terminal bronchiolar epithelium detected a wave of proliferation that was initiated 72 hours after naphthalene injury and subsided by 240 hours (Fig. 6). In contrast, proliferation of $Catnb^{\Delta E3}$ epithelial cells was consistently increased by 36 hours. Proliferation peaked in animals of either genotype at 72 hours and returned to normal at 240 hours. The instantaneous proliferative index for wild-type and $Catnb^{\Delta E3}$ epithelium was indistinguishable at the 18-hour ($p = .25$) and 240-hour ($p = .23$) recovery time points. These data demonstrated that cells of both genotypes are competent to respond to stimuli that initiate and terminate the proliferative response to injury. A significant increase in proliferative index was identified in $Catnb^{\Delta E3}$ airways at the 36-hour ($p = .04$) and 72-hour ($p = .002$) time points. Phenotypic analysis of cells that proliferated in response to naphthalene treatment demonstrated that the majority of BrdU-labeled cells were CCSP-immunoreactive and that their representation within the total proliferative pool did not vary by genotype (Fig. 6). These data suggested that β-catenin stabilization resulted in an increase in the number of naphthalene-resistant, proliferative cells and suggested that amplification of the reparative cell pool was the basis for enhanced repair of the $Catnb^{\Delta E3}$ epithelium.

Depletion of the Ciliated Cell Population Within Repairing Epithelium—Previous analysis indicated that *β*-catenin stabilization altered the differentiated characteristics (Figs. 1, 2) and differentiation potential of CCSP-expressing cells in the steady state (Fig. 4) and that these cells self-renewed in the context of repair (Fig. 5). To determine the differentiation potential of cells that proliferate in response to naphthalene injury, FoxJ1 mRNA abundance was analyzed by quantitative RT-PCR (Fig. 7). Messenger RNA abundance at the 8-day recovery time point was 1.969 ± 0.387 for the wild-type lung and 0.958 ± 0.270 in the $Catnb^{\Delta E3}$ lung, and differences were statistically significant ($p = .05$; data not shown). To further assess the differentiation potential of the naphthalene-resistant progenitor cell population, representation of FoxJ1-expressing cells in nascent epithelium of wild-type and $Catnb^{\Delta E3}$ was determined. Since Clara cell proliferation is associated with differentiation of some daughter cells into ciliated cells [5] and ciliated cells did not proliferate in response to naphthalene injury (Fig. 6), continuous BrdU labeling was used to distinguish nascent versus pre-existing FoxJ1-immunoreactive ciliated cells (Fig. 7). In the wild-type epithelium, nascent ciliated cells were 14.95% ± 0.53% of total epithelial cells, whereas they were 1.05% ± 0.12% of epithelial cells in the $Catnb^{\Delta E3}$ epithelium. These data further reinforce the conclusion that stabilization of *β*-catenin in CCSP-expressing cells attenuates secretory to ciliated cell differentiation.

Discussion

The demonstration by others and us that TOPGal transgene activation indicative of *β*-catenin signaling is dynamically regulated in airways during lung development suggests important roles for this pathway in coordination of branching and/or differentiation of lung endoderm [26–28,53]. Genetic manipulation indicates that low Wnt/*β*-catenin signaling favors establishment of the lung anlagen on dpc 9.5 and is followed by high levels of Wnt/-*β*-catenin signaling during the period of branching morphogenesis (dpc 9.5–12.5). Following establishment of the airway, Wnt/*β*-catenin signaling is attenuated in centrilobar regions ~dpc 13.5 and gradually recedes along the proximal-to-distal axis during the remainder of lung development [26,53] (supplemental online Fig. 2). It is well established that epithelial differentiation in the developing airway proceeds in a proximal-to-distal wave that accompanies specification of proximal versus distal lineages [13,37,38]. Our observation of a reciprocal relationship between downregulation of reporter gene expression from the TOPGal transgene and appearance of early secretory cell precursors is consistent with roles for *β*-catenin signaling in regulation of these processes.

Ultrastructural and molecular properties of nonciliated epithelial cells lining bronchioles of $Catnb^{\Delta E3}$ mice were distinct from those of mature Clara cells that normally reside in bronchioles of wild-type mice. Clara cells of the steady-state bronchiolar epithelium are characterized by a high cytoplasmic-to-nuclear ratio, abundant secretory granules, high-level expression of Clara cell differentiation markers, and sensitivity to naphthalene [8,9,54,55]. Even though Clara cells of the steady-state airway exhibit differentiated features, their phenotype changes dramatically upon entry into the cell cycle. Actively proliferating Clara cells, referred to as type A Clara cells, lack secretory granules and smooth endoplasmic reticulum [4]. The proliferative quiescence of nonciliated cells of the steady-state $Catnb^{\Delta E3}$ airway distinguished them from the mitotic type A cell of the repairing wild-type airway. Only bronchiolar stem cells have the properties of less differentiated character, naphthalene resistance, and infrequent proliferation that are observed among nonciliated cells in bronchioles of $Catnb^{\Delta E3}$ mice [2,3,11]. On the basis of these observations, we conclude that nonciliated cells lining bronchioles of $Catnb^{\Delta E3}$ mice represent supernumerary bronchiolar stem cells whose differentiation is arrested through constitutive expression of stabilized *β*-catenin.

Bronchiolar stem cells reside in close apposition to pulmonary neuroendocrine cells within neuroepithelial bodies and at the bronchoalveolar duct junction [2,3]. Their appearance during lung development is less well understood. Cells that expressed truncated *β*-catenin were remarkably similar to a unique population of neuroepithelial body (NEB) associated cells that are segregated during lung development. These cells were originally termed Clara-like cells [56] and were found to express CCSP [57] but were distinguished from surrounding CCSP-expressing cells by their low cytoplasmic-to-nuclear ratio [58]. The structural, phenotypic, and functional similarities between cells expressing truncated *β*-catenin and NEB-associated cells suggest that *β*-catenin signaling (or a pathway that mimics this process) functions in the maintenance of this immature cell type. We suggest that potentiation of *β*-catenin during the period of airway cell differentiation inhibits differentiation to a Clara cell phenotype. Similarly, depletion of the ciliated cell population can be attributed to a deficiency in the precursor to this cell type, the Clara cell. Hyperplasia of an undifferentiated, quiescent, naphthalene-resistant cell with properties of the bronchiolar stem cell suggests that differentiation status is the critical distinction between the bronchiolar stem cell and the facultative TAC. Our findings suggest that downregulation of *β*-catenin signaling during lung maturation is a prerequisite for differentiation of endodermal precursor cells into the facultative TAC and differentiated ciliated cells. We speculate that sequestration of the bronchiolar stem cell requires extrinsic signaling cues provided by the stem cell niche. Constitutive potentiation of *β*-catenin signaling beyond the developmental stage at which this pathway is typically downregulated leads to niche-independent expansion of cells with properties of the bronchiolar stem cell.

We present data demonstrating that supernumerary bronchiolar stem cells generated through stabilization of *β*-catenin are quiescent in the steady state and responsive to mitotic cues generated within injured airways. This observation is in stark contrast to events occurring within rapidly renewing tissues following activation of *β*-catenin signaling. Cells within rapidly renewing tissues, such as those of the gut and hematopoietic systems, are positioned within the stem cell hierarchy according to their unique proliferative, migratory, and differentiation potentials [14,15]. However, the recent demonstration that intestinal stem cells proliferate frequently, like their TAC progeny [59], suggests that longevity of the TSC must be attributed to mechanisms other than cell cycle frequency. The critical difference between TSC and TAC may be their relative level of commitment to the differentiation program. Accordingly, TSC would be maintained over the life span of the organism because they do not differentiate. In contrast, TAC have a finite life span, their daughters eventually committing to programs of differentiation giving rise to either villus or Paneth lineages. Genetic manipulation of *β*-catenin stability within rapidly renewing tissues supports a critical role for Wnt/*β*-catenin signaling in regulation of the mitotic compartment. However, our demonstration that stabilized *β*-catenin negatively regulates bronchiolar stem/progenitor cell differentiation without increasing the rate of cell proliferation suggests an alternative role for active *β*-catenin in the modulation of the stem cell compartment. We propose that *β*-catenin-mediated inhibition of either TSC or TAC differentiation increases the number of cells capable of responding to mitotic signals. Accordingly, the impact of *β*-catenin stabilization varies with the mitotic status of the tissue. In rapidly renewing tissues, such as the gut, stabilization of *β*-catenin leads to uncontrolled expansion of cells whose differentiation into postmitotic progeny is arrested. In contrast, potentiation of *β*-catenin signaling within slowly renewing tissues arrests the differentiation of TSC/TAC without further proliferative expansion because of the absence of local mitotic cues.

Conclusion

We have determined that downregulation of *β*-catenin signaling is necessary for establishment of the bronchiolar stem cell hierarchy. Potentiation of signaling through expression of an N-terminally truncated *β*-catenin resulted in a dramatic reduction in the abundance of two derivatives of the bronchiolar stem cell, the differentiated secretory (Clara) cell and the

terminally differentiated (ciliated) cell. The lack of differentiated cell types was accompanied by a corresponding increase in the number of phenotypically, molecularly, and functionally immature epithelial cells. Such cells were quiescent in the steady state but retained the capacity to proliferate following airway injury. However, reduced differentiation of daughter cells following injury resulted in further depletion of mature cell types, including Clara and ciliated cells. Thus, the failure to attenuate β-catenin signaling during the late prenatal/early postnatal period generated a population of cells that exhibited all of the known characteristics of the bronchiolar stem cell, except that that they failed to generate differentiated epithelial cell types. These data indicate that β-catenin signaling functions primarily as a negative regulator of bronchiolar cell differentiation. We suggest that attenuation of β-catenin signaling during the late prenatal/early postnatal period promotes establishment of the bronchiolar stem cell hierarchy by promoting TAC differentiation. Thus, the chief distinction between the bronchiolar TSC and TAC is their relative receptivity to differentiation signals. The negative impact of β-catenin signaling on differentiation has important implications for understanding the relationship between developmental progenitor cells and adult tissue stem cells and the signals that segregate mitotically competent cells into TSC and TAC phenotypes. We suggest that transitions in β-catenin signaling serve to establish the TSC and TAC pools and that the principal distinction between these two cell types is their susceptibility to differentiation signals.

Supplementary Material

Refer to Web version on PubMed Central for supplementary material.

Acknowledgments

We thank Dr. E. Fuchs for TOPGal/Cd1 mice and Dr. J. Whitsett for *Catnb*$^{flox(E3)}$ mice (with the permission of M.M. Taketo). We are indebted to Christine Burton for assistance with animal husbandry and Dr. Donna Stolz and Katherine A. Clarke in the University of Pittsburgh Center for Biologic Imaging for electron microscopy. This research was supported by the National Heart, Lung, and Blood Institute of the National Institutes of Health.

References

1. Reynolds SD, Reynolds PR, Snyder JC, et al. CCSP regulates cross talk between secretory cells and both ciliated cells and macrophages of the conducting airway. Am J Physiol Lung Cell Mol Physiol 2007;293:L114–L123. [PubMed: 17384087]
2. Giangreco A, Reynolds SD, Stripp BR. Terminal bronchioles harbor a unique airway stem cell population that localizes to the bronchoalveolar duct junction. Am J Pathol 2002;161:173–182. [PubMed: 12107102]
3. Hong KU, Reynolds SD, Giangreco A, et al. Clara cell secretory protein-expressing cells of the airway neuroepithelial body microenvironment include a label-retaining subset and are critical for epithelial renewal after progenitor cell depletion. Am J Respir Cell Mol Biol 2001;24:671–681. [PubMed: 11415931]
4. Evans MJ, Johnson LV, Stephens RJ, et al. Renewal of the terminal bronchiolar epithelium in the rat following exposure to NO2 or O3. Lab Invest 1976;35:246–257. [PubMed: 957607]
5. Evans MJ, Cabral-Anderson LJ, Freeman G. Role of the Clara cell in renewal of the bronchiolar epithelium. Lab Invest 1978;38:648–653. [PubMed: 661220]
6. Sell S. Heterogeneity and plasticity of hepatocyte lineage cells. Hepatology 2001;33:738–750. [PubMed: 11230756]
7. Kawasaki E, Abiru N, Eguchi K. Prevention of type 1 diabetes: From the view point of beta cell damage. Diabetes Res Clin Pract 2004;66(suppl 1):S27–S32. [PubMed: 15563975]
8. Mahvi D, Bank H, Harley R. Morphology of a naphthalene-induced bronchiolar lesion. Am J Pathol 1977;86:558–572. [PubMed: 842612]

9. Plopper CG, Suverkropp C, Morin D, et al. Relationship of cytochrome P-450 activity to Clara cell cytotoxicity. I. Histopathologic comparison of the respiratory tract of mice, rats and hamsters after parenteral administration of naphthalene. J Pharmacol Exp Ther 1992;261:353–363. [PubMed: 1560379]
10. Stripp BR, Maxson K, Mera R, et al. Plasticity of airway cell proliferation and gene expression after acute naphthalene injury. Am J Physiol 1995;269:L791–L799. [PubMed: 8572241]
11. Reynolds SD, Giangreco A, Power JH, et al. Neuroepithelial bodies of pulmonary airways serve as a reservoir of progenitor cells capable of epithelial regeneration. Am J Pathol 2000;156:269–278. [PubMed: 10623675]
12. Kim CF, Jackson EL, Woolfenden AE, et al. Identification of bronchioalveolar stem cells in normal lung and lung cancer. Cell 2005;121:823–835. [PubMed: 15960971]
13. Wert SE, Glasser SW, Korfhagen TR, et al. Transcriptional elements from the human SP-C gene direct expression in the primordial respiratory epithelium of transgenic mice. Dev Biol 1993;156:426–443. [PubMed: 8462742]
14. Alison MR, Poulsom R, Forbes S, et al. An introduction to stem cells. J Pathol 2002;197:419–423. [PubMed: 12115858]
15. Potten CS, Loeffler M. Stem cells: Attributes, cycles, spirals, pitfalls and uncertainties. Lessons for and from the crypt. Development 1990;110:1001–1020. [PubMed: 2100251]
16. Radtke F, Clevers H, Riccio O. From gut homeostasis to cancer. Curr Mol Med 2006;6:275–289. [PubMed: 16712475]
17. Sansom OJ, Reed KR, Hayes AJ, et al. Loss of Apc in vivo immediately perturbs Wnt signaling, differentiation, and migration. Genes Dev 2004;18:1385–1390. [PubMed: 15198980]
18. Kirstetter P, Anderson K, Porse BT, et al. Activation of the canonical Wnt pathway leads to loss of hematopoietic stem cell repopulation and multilineage differentiation block. Nat Immunol 2006;7:1048–1056. [PubMed: 16951689]
19. Scheller M, Huelsken J, Rosenbauer F, et al. Hematopoietic stem cell and multilineage defects generated by constitutive beta-catenin activation. Nat Immunol 2006;7:1037–1047. [PubMed: 16951686]
20. Trowbridge JJ, Xenocostas A, Moon RT, et al. Glycogen synthase kinase-3 is an in vivo regulator of hematopoietic stem cell repopulation. Nat Med 2006;12:89–98. [PubMed: 16341242]
21. Reya T, Duncan AW, Ailles L, et al. A role for Wnt signalling in self-renewal of haematopoietic stem cells. Nature 2003;423:409–414. [PubMed: 12717450]
22. Gat U, DasGupta R, Degenstein L, et al. De Novo hair follicle morphogenesis and hair tumors in mice expressing a truncated beta-catenin in skin. Cell 1998;95:605–614. [PubMed: 9845363]
23. Huelsken J, Vogel R, Erdmann B, et al. beta-Catenin controls hair follicle morphogenesis and stem cell differentiation in the skin. Cell 2001;105:533–545. [PubMed: 11371349]
24. Millar SE, Willert K, Salinas PC, et al. WNT signaling in the control of hair growth and structure. Dev Biol 1999;207:133–149. [PubMed: 10049570]
25. Lo Celso C, Prowse DM, Watt FM. Transient activation of beta-catenin signalling in adult mouse epidermis is sufficient to induce new hair follicles but continuous activation is required to maintain hair follicle tumours. Development 2004;131:1787–1799. [PubMed: 15084463]
26. Okubo T, Hogan BL. Hyperactive Wnt signaling changes the developmental potential of embryonic lung endoderm. J Biol 2004;3:11. [PubMed: 15186480]
27. Mucenski ML, Wert SE, Nation JM, et al. beta-Catenin is required for specification of proximal/distal cell fate during lung morphogenesis. J Biol Chem 2003;278:40231–40238. [PubMed: 12885771]
28. Shu W, Guttentag S, Wang Z, et al. Wnt/beta-catenin signaling acts upstream of N-myc, BMP4, and FGF signaling to regulate proximal-distal patterning in the lung. Dev Biol 2005;283:226–239. [PubMed: 15907834]
29. Chomczynski P, Sacchi N. Single-step method of RNA isolation by acid guanidinium thiocyanate-phenol-chloroform extraction. Anal Biochem 1987;162:156–159. [PubMed: 2440339]
30. DasGupta R, Fuchs E. Multiple roles for activated LEF/TCF transcription complexes during hair follicle development and differentiation. Development 1999;126:4557–4568. [PubMed: 10498690]

31. Stolz DB, Ross MA, Salem HM, et al. Cationic colloidal silica membrane perturbation as a means of examining changes at the sinusoidal surface during liver regeneration. Am J Pathol 1999;155:1487–1498. [PubMed: 10550305]
32. Reynolds SD, Shen H, Reynolds PR, et al. Molecular and functional properties of lung side population cells. Am J Physiol Lung Cell Mol Physiol 2007;292:L972–L983. [PubMed: 17142352]
33. Heid CA, Stevens J, Livak KJ, et al. Real time quantitative PCR. Genome Res 1996;6:986–994. [PubMed: 8908518]
34. Chichester CH, Philpot RM, Weir AJ, et al. Characterization of the cytochrome P-450 monooxygenase system in nonciliated bronchiolar epithelial (Clara) cells isolated from mouse lung. Am J Respir Cell Mol Biol 1991;4:179–186. [PubMed: 1991074]
35. Taswell C. Limiting dilution assays for the determination of immunocompetent cell frequencies. I. Data analysis. J Immunol 1981;126:1614–1619. [PubMed: 7009746]
36. You Y, Huang T, Richer EJ, et al. Role of f-box factor foxj1 in differentiation of ciliated airway epithelial cells. Am J Physiol Lung Cell Mol Physiol 2004;286:L650–L657. [PubMed: 12818891]
37. Shannon JM, Nielsen LD, Gebb SA, et al. Mesenchyme specifies epithelial differentiation in reciprocal recombinants of embryonic lung and trachea. Dev Dyn 1998;212:482–494. [PubMed: 9707322]
38. Rawlins EL, Ostrowski LE, Randell SH, et al. Lung development and repair: Contribution of the ciliated lineage. Proc Natl Acad Sci U S A 2007;104:410–417. [PubMed: 17194755]
39. Wuenschell CW, Sunday ME, Singh G, et al. Embryonic mouse lung epithelial progenitor cells co-express immunohistochemical markers of diverse mature cell lineages. J Histochem Cytochem 1996;44:113–123. [PubMed: 8609367]
40. DasGupta R, Rhee H, Fuchs E. A developmental conundrum: A stabilized form of beta-catenin lacking the transcriptional activation domain triggers features of hair cell fate in epidermal cells and epidermal cell fate in hair follicle cells. J Cell Biol 2002;158:331–344. [PubMed: 12135986]
41. Soriano P. Generalized lacZ expression with the ROSA26 Cre reporter strain. Nat Genet 1999;21:70–71. [PubMed: 9916792]
42. Harada N, Tamai Y, Ishikawa T, et al. Intestinal polyposis in mice with a dominant stable mutation of the beta-catenin gene. EMBO J 1999;18:5931–5942. [PubMed: 10545105]
43. Simon DM, Arikan MC, Srisuma S, et al. Epithelial cell PPARgamma is an endogenous regulator of normal lung maturation and maintenance. Proc Am Thorac Soc 2006;3:510–511. [PubMed: 16921131]
44. Cardoso WV, Stewart LG, Pinkerton KE, et al. Secretory product expression during Clara cell differentiation in the rabbit and rat. Am J Physiol 1993;264:L543–L552. [PubMed: 8333547]
45. Plopper CG, Alley JL, Serabjitsingh CJ, et al. Cytodifferentiation of the nonciliated bronchiolar epithelial (Clara) cell during rabbit lung maturation: An ultrastructural and morphometric study. Am J Anat 1983;167:329–357. [PubMed: 6881072]
46. Mucenski ML, Nation JM, Thitoff AR, et al. Beta-catenin regulates differentiation of respiratory epithelial cells in vivo. Am J Physiol Lung Cell Mol Physiol 2005;289:L971–L979. [PubMed: 16040629]
47. Reynolds SD, Hong KU, Giangreco A, et al. Conditional Clara cell ablation reveals a self-renewing progenitor function of pulmonary neuroendocrine cells. Am J Physiol Lung Cell Mol Physiol 2000;278:L1256–L1263. [PubMed: 10835332]
48. Linnoila RI. Functional facets of the pulmonary neuroendocrine system. Lab Invest 2006;86:425–444. [PubMed: 16568108]
49. Jones PH, Watt FM. Separation of human epidermal stem cells from transit amplifying cells on the basis of differences in integrin function and expression. Cell 1993;73:713–724. [PubMed: 8500165]
50. Jones PH, Harper S, Watt FM. Stem cell patterning and fate in human epidermis. Cell 1995;80:83–93. [PubMed: 7813021]
51. Kobayashi K, Rochat A, Barrandon Y. Segregation of keratinocyte colony-forming cells in the bulge of the rat vibrissa. Proc Natl Acad Sci U S A 1993;90:7391–7395. [PubMed: 8346261]
52. Rawlins EL, Hogan BL. Epithelial stem cells of the lung: Privileged few or opportunities for many? Development 2006;133:2455–2465. [PubMed: 16735479]

53. Dean CH, Miller LA, Smith AN, et al. Canonical Wnt signaling negatively regulates branching morphogenesis of the lung and lacrimal gland. Dev Biol 2005;286:270–286. [PubMed: 16126193]

54. Plopper CG, Macklin J, Nishio SJ, et al. Relationship of cytochrome P-450 activity to Clara cell cytotoxicity. III. Morphometric comparison of changes in the epithelial populations of terminal bronchioles and lobar bronchi in mice, hamsters, and rats after parenteral administration of naphthalene. Lab Invest 1992;67:553–565. [PubMed: 1434534]

55. Stripp, BR.; Reynolds, SD. Clara cells. In: Shapiro, S.; Laurent, G., editors. Encyclopedia of Respiratory Medicine. St. Louis: Elsevier; 2006. p. 471-477.

56. Haller CJ. A scanning and transmission electron microscopic study of the development of the surface structure of neuroepithelial bodies in the mouse lung. Micron 1994;25:527–538. [PubMed: 7881894]

57. Khoor A, Gray ME, Singh G, et al. Ontogeny of Clara cell-specific protein and its mRNA: Their association with neuroepithelial bodies in human fetal lung and in bronchopulmonary dysplasia. J Histochem Cytochem 1996;44:1429–1438. [PubMed: 8985135]

58. Cutz E. Neuroendocrine cells of the lung. An overview of morphologic characteristics and development. Exp Lung Res 1982;3:185–208. [PubMed: 6188605]

59. Barker N, van Es JH, Kuipers J, et al. Identification of stem cells in small intestine and colon by marker gene Lgr5. Nature 2007;449:1003–1007. [PubMed: 17934449]

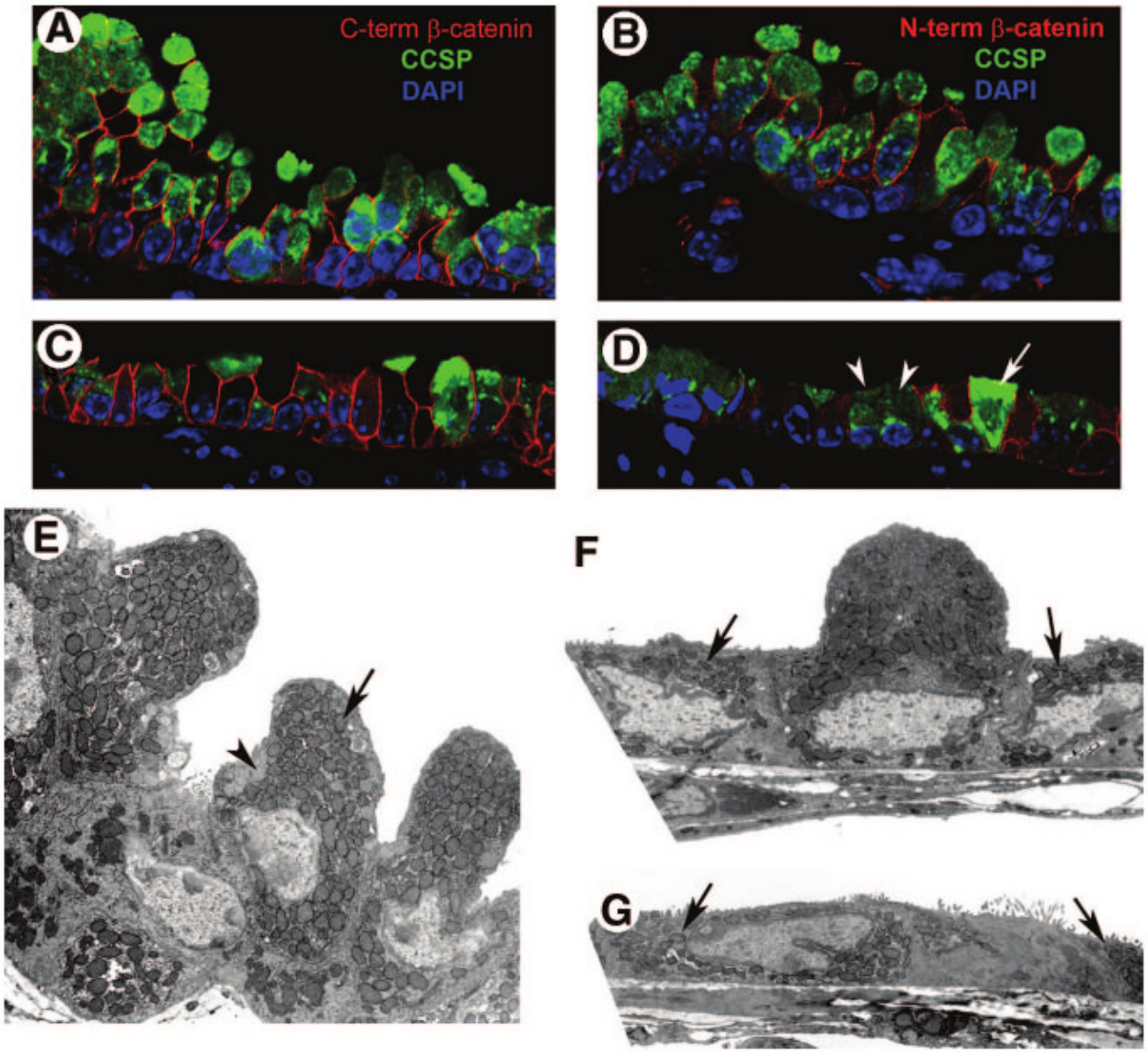

Figure 1.

Steady-state epithelial cell phenotype and ultrastructure. **(A–D):** Analysis of cellular morphology. Lung tissue from steady-state wild-type **(A, B)** or Catnb$^{\Delta E3}$ **(C, D)** mice was dual immunostained for CCSP (green) and a C-term epitope of *β*-catenin (red) **(A, C)** or N-term epitope specific to wild-type *β*-catenin (red) **(B, D)**. Tissue was counterstained with DAPI (blue). Confocal microscopy was used to image representative regions of the bronchiolar epithelium at ×120. Arrows in **(D)** indicate nonrecombined cells, and arrowheads indicate recombined cells. **(E–G):** Analysis of ultrastructure. Wild-type **(E)** and Catnb$^{\Delta E3}$ **(F, G)** tissue was analyzed by transmission electron microscopy, and representative images of Clara cells are presented at ×8,000. Arrow and arrowhead in (**E**) identify mitochondria and secretory granules, respectively, of normal Clara cells. Arrows in (**F**) and (**G**) indicate morphologically immature cells. Abbreviations: CCSP, Clara cell secretory protein; C-term, C-terminal; DAPI, 4,6-diamidino-2-phenylindole; N-term, N-terminal.

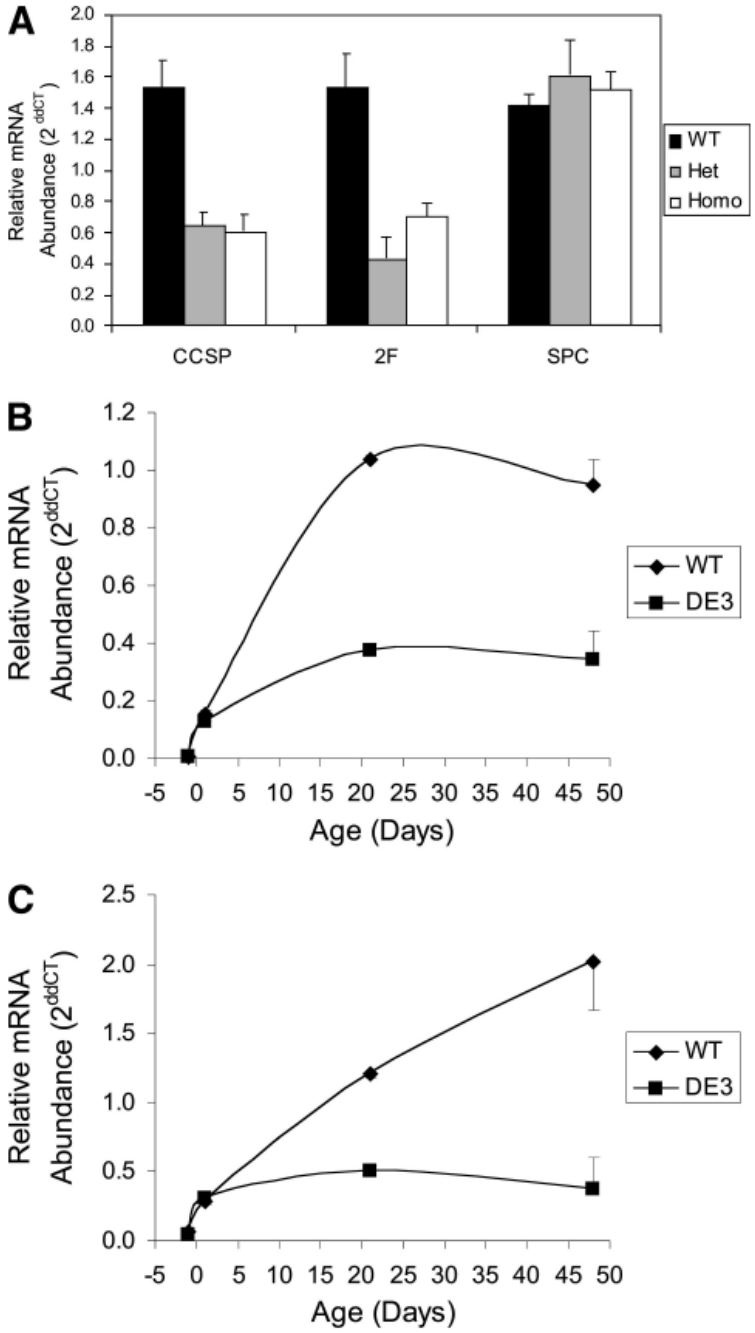

Figure 2.

Gene expression as a function of zygosity and age. **(A):** Total lung RNA from WT (black bars), Het DE3 (medium gray bars), and Homo DE3 (white bars) mice was assayed for expression of CCSP, 2F, and SPC by quantitative reverse transcription-polymerase chain reaction, and average ddC_T values are presented ± SEM. Genotype-dependent differences were noted for expression of CCSP and 2F. **(B, C):** Gene expression as a function of age. CCSP **(B)** and 2F **(C)** mRNA abundance was assessed in total lung RNA from WT and DE3 mice at days post coitum 17.5 and postnatal days 1, 21, and 48. Data are presented as the average ddC_T ± SEM. Genotype-dependent differences in CCSP and 2F mRNA abundance were noted at postnatal days 21 and 48. Abbreviations: 2F, cytochrome P450-2F2; CCSP, Clara cell secretory protein;

ddCT, $\Delta\Delta C_T$; DE3, Catnb$^{\Delta E3}$; Het, heterozygous; Homo, homozygous; SPC, surfactant protein C; WT, wild-type.

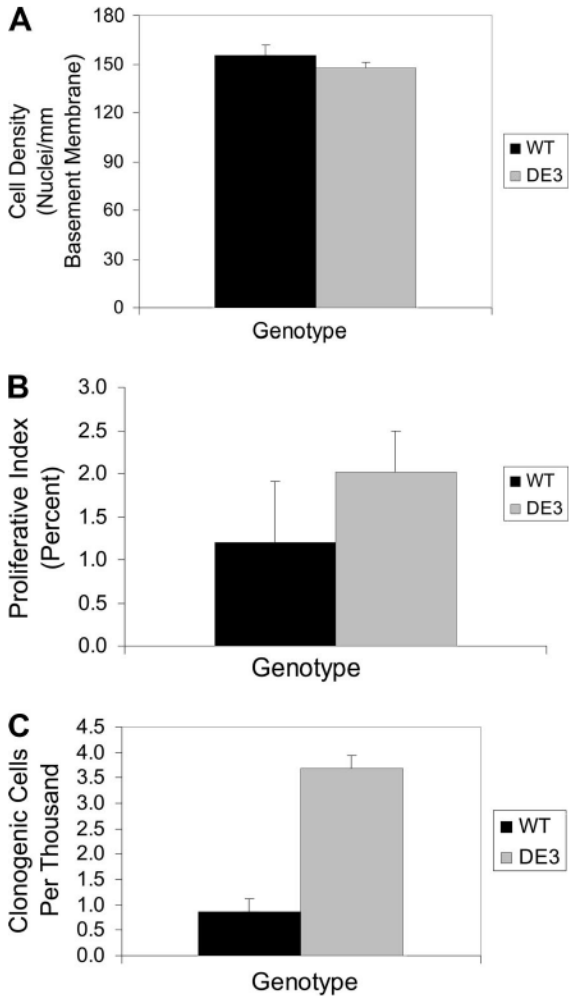

Figure 3.

Cell density, proliferation, and clonogenic frequency. **(A):** Analysis of cell density. Epithelial cell density for WT (black bar) and DE3 (gray bar) mice was reported as the number of nuclei per millimeter of basement membrane ± SEM. Cell density did not vary by genotype. **(B):** Analysis of steady-state proliferation. The cumulative proliferative index for WT (black bar) and DE3 (gray bar) mice was reported as average values ± SEM. Proliferative index did not vary by genotype. **(C):** Analysis of clonogenic frequency. The frequency of clonogenic cells in airway epithelial cell preparations from WT (black bar) or DE3 (gray bar) littermates was assayed in the steady state. Data are presented as the mean ± SEM. Genotype-dependent differences were detected. Abbreviations: DE3, Catnb$^{\Delta E3}$; WT, wild-type.

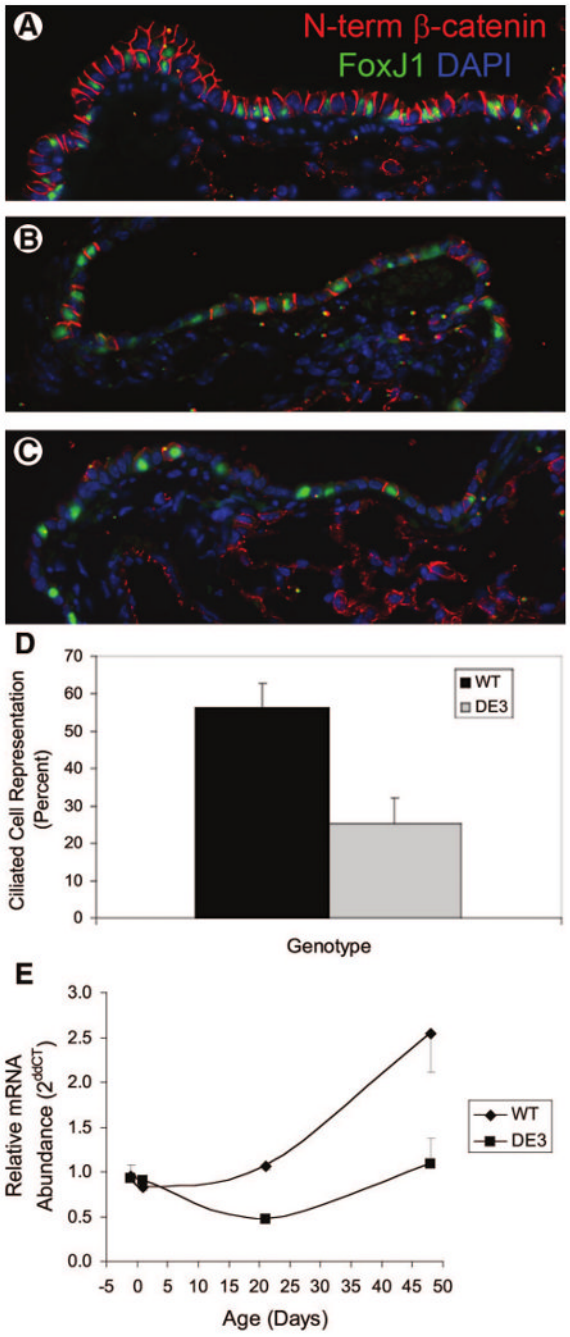

Figure 4.

Ciliated cell differentiation. **(A–C):** Histological analysis. Lung tissue from steady-state WT **(A)** or DE3 **(B, C)** mice was dual immunostained for FoxJ1 (green) and an N-term epitope specific to WT *β*-catenin (red). Tissue was counterstained with DAPI (blue). **(D):** Ciliated cell abundance. The representation of ciliated cells among all epithelial cells was determined in WT (black bar) and DE3 (gray bar) mice. Genotype-dependent differences were noted. **(E):** Gene expression as a function of age. FoxJ1 mRNA abundance was assessed in total lung RNA from WT and DE3 mice at day post coitum 17.5 and postnatal days 1, 21, and 48. Data are presented as the average ddCT ± SEM. Genotype-dependent differences were noted at postnatal

days 21 and 48. Abbreviations: DAPI, 4,6-diamidino-2-phenylindole; ddCT, $\Delta\Delta C_T$; DE3, $Catnb^{\Delta E3}$; N-term, N-terminal; WT, wild-type.

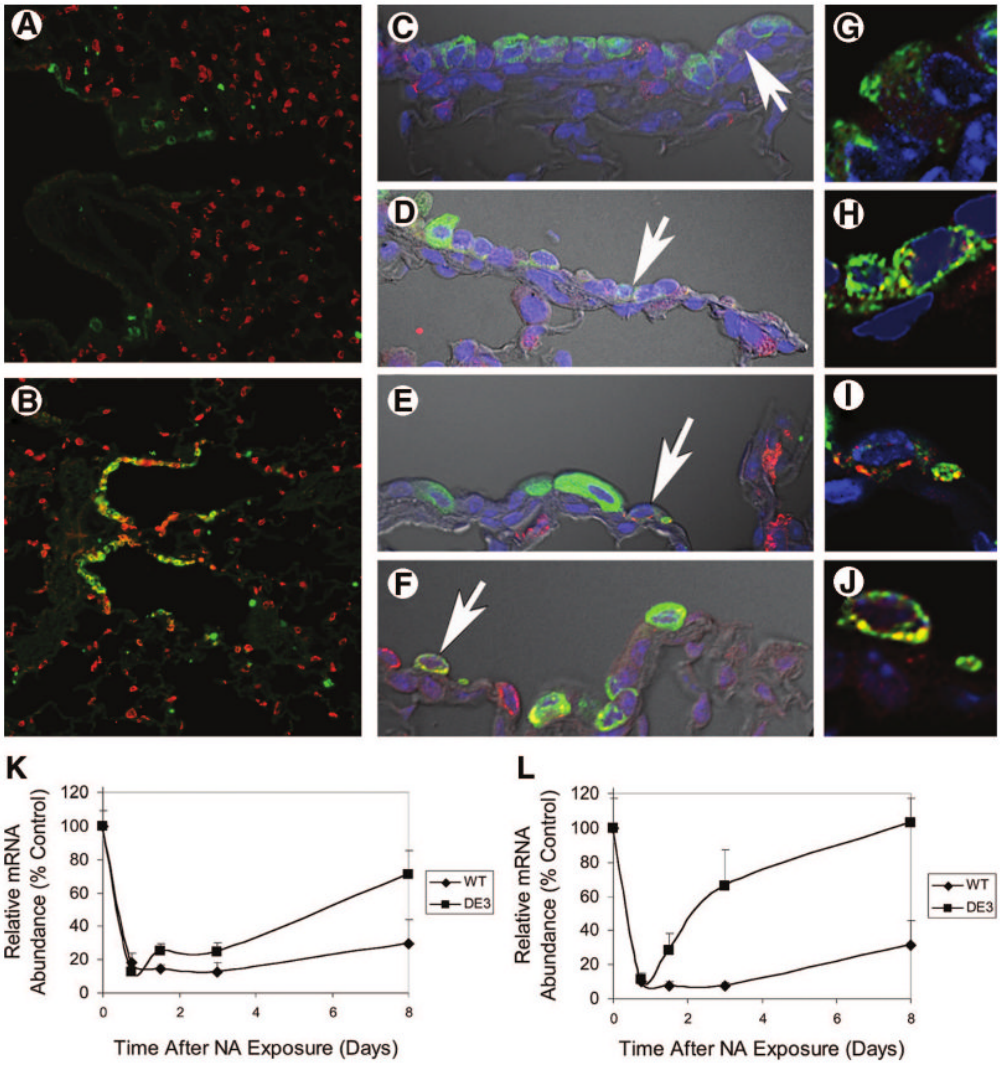

Figure 5.

Molecular phenotype of reparative cells. **(A, B):** Expression of Clara cell secretory protein (CCSP) and prosurfactant protein C (proSPC) in WT **(A)** and DE3 **(B)** mice treated with naphthalene and allowed to recover for 3 days. Lung tissue was stained with CCSP (green) and proSPC (red). Representative images of terminal bronchioles were captured using standard fluorescence microscopy and are presented at ×20. **(C–J):** Confocal microscopy was used to colocalize CCSP (green) and proSPC (red) in control WT **(C, G)** and DE3 **(D, H)** mice and NA-treated WT **(E, I)** and DE3 **(F, J)** mice on recovery day 3. Representative images are shown at ×120 **(C–F)** or at ×1,000 **(G–J)**. Arrows indicate cells that are dual-positive for CCSP and proSPC. **(K, L):** Gene expression as a function of recovery time. WT or DE3 mice were treated with NA and allowed to recover for 0.75, 1.5, 3, or 8 days. Total lung RNA from untreated control (0) and treated mice was assayed for expression of CCSP **(K)** and cytochrome P450-2F2 **(L)** by quantitative reverse transcription-polymerase chain reaction. Data are presented as the percentage of control values ± SEM. Genotype-dependent differences were noted for expression of CCSP and cytochrome P450-2F2 at the 8-day time point. Abbreviations: DE3, Catnb$^{\Delta E3}$; NA, naphthalene; WT, wild-type.

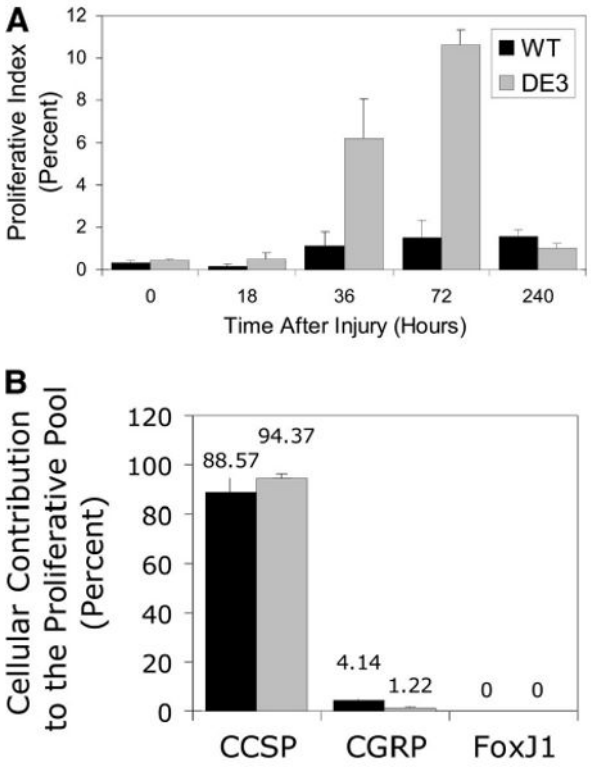

Figure 6.

Proliferation and molecular phenotype of S-phase cells. **(A):** The instantaneous proliferative index for WT (black bars) and DE3 (gray bars) mice was reported as average values ± SEM. Significant effects of time and genotype were detected and are detailed in Results. **(B):** Analysis of proliferative cell phenotype. The contribution of secretory cells (CCSP), pulmonary neuroendocrine cells (CGRP), and ciliated cells (FoxJ1) to the mitotic pool was determined and reported as average ± SEM. WT, black bars; DE3, gray bars. Genotype-dependent differences were not detected. Abbreviations: CCSP, Clara cell secretory protein; CGRP, calcitonin gene-related peptide; DE3, $Catnb^{\Delta E3}$; WT, wild-type.

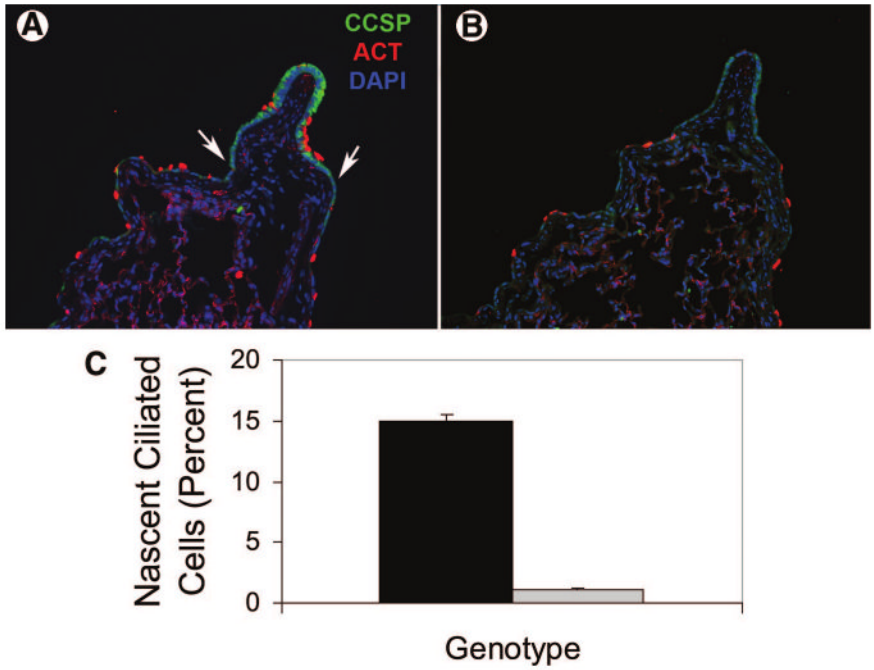

Figure 7.

Ciliated cell regeneration. **(A, B):** Ciliated cell phenotypes within regenerative zones. Wild-type **(A)** and DE3 were treated with naphthalene and allowed to recover for 3 days. Ciliated and Clara cells were detected by dual immunofluorescence analysis of CCSP (green) and ACT (red), and nuclei were counterstained with DAPI (blue). Arrows demarcate the regenerative zone. **(C):** Analysis of ciliated cell differentiation. Nascent ciliated cells were defined as FoxJ1/bromodeoxyuridine dual immunopositive cells and were quantified as a percentage of total FoxJ1 immunopositive cells in wild-type (black bar) and DE3 (gray bar) tissue on recovery day 8. Differences were statistically significant. Abbreviations: ACT, acetylated tubulin; CCSP, Clara cell secretory protein; DAPI, 4,6-diamidino-2-phenylindole; DE3, $Catnb^{\Delta E3}$.